

VOLTAGE SAG MITIGATION USING A NEW DIRECT CONTROL IN D-STATCOM FOR DISTRIBUTION SYSTEMS

Rahmat-Allah HOOSHMAND¹, Mahdi BANEJAD², Mostafa AZIMI³

With the growth of need of electrical energy in the technological societies, the demand for receiving the high quality electrical energy is being increased. Among the different disturbances affecting the power quality, the voltage sag and temporary voltage are essential issues especially that need to be fully investigated in the automated systems. In this paper, firstly, the effects of voltage sag due to three phase short circuit, starting of induction motor and transformer energizing are studied. Then, influence of voltage sag compensation by means of distribution synchronous compensator (D-Statcom) is investigated. After that, a method, namely direct control is presented for this compensator. The method measures the active and reactive powers simultaneously to control directly the switching patterns in the D-Statcom. The proposed direct control system is capable to minimize the power interruption and voltage sag and it is independent of system parameters using direct control. The method is then simulated on an IEEE standard-test system using PSCAD/EMTC software. The results of the simulation shows the proposed method in control strategy is able to compensate voltage sag.

Keywords: Voltage Sag, Distribution Synchronous Compensators (D-Statcom), Active and Reactive Power Control

1. Introduction

One of the power system problem related to the power quality is voltage sag. Around 80% of the power quality problem is related to the voltage sag [1]. According to IEEE standard 1159-1995, the voltage sag is the temporary voltage drop between 10 to 90% of the effective voltage in the power frequency for the duration of half cycle to one minute [2-3]. There are several reasons for occurrence of voltage sag in the power systems such as short circuits, start-up of large induction motors, sudden load changes and transformer energization [4-7]. Due to the nature of the voltage sag, this phenomenon lies in the transient category. The phenomena causing voltage are also classified into low or mid-frequency transients.

¹ Associate Prof., Dept. of Electrical Engineering, University of Isfahan, Isfahan, Iran, hooshmand_r@yahoo.com

² Associate Prof., Elec. And Robotic Engineering Faculty, Shahrood University of Technology, Iran

³ Eng., Dept. of Electrical Engineering, University of Isfahan, Isfahan, Iran

Nowadays, sensitive equipments are being used in industries and the voltage sag in the power system is not acceptable. There are several methods that are being used to reduce the voltage sag. In some methods, compensators based on the voltage and current source are used [8]. One of the other compensator is distribution synchronous static compensators (D-Statcom) [9]. This parallel voltage compensator is used to decrease the voltage sag. In addition, it can be used for damping active and reactive power oscillations as well as mitigation of harmonic currents of the loads [10]. In this compensator, the voltage sag is compensated by means of reactive power using d-q conventional method [8-9].

In this paper, the issue of the voltage sag is reviewed briefly in section 2. The proposed method in compensating the voltage sag using D-Statcom is explained in Section 3. In this section, a new direct control of D-Statcom is also introduced. Since in the proposed control system of D-Statcom, the active and reactive powers are sampled separately, the compensation of the voltage sag and voltage disruption is performed in the desired level. The proposed control is then simulated on the IEEE 13-Bus test system. In the simulation, the compensation is compared with the conventional d-q control methods. The results of the simulation validate the proposed method.

2. Creating factors of voltage sag

2.1. Short circuit faults

Among Symmetrical and unsymmetrical short circuits, three phase short circuit has the most effect on the voltage sag [2, 11-12]. In order to determine the amount of the voltage sag in the radial model of the distribution system, the voltage divider model can be used as illustrated in Fig. 1. In this figure, impedance Z_s is the source impedance at the point of common coupling (PCC) and Z_F is the impedance between the PCC and fault point. The voltage at PCC bus can be obtained from [2]:

$$V_{sag} = \frac{Z_F}{Z_S + Z_F} E \quad (1)$$

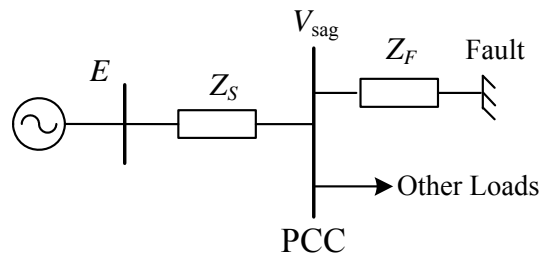


Fig. 1. Voltage divider model for computing voltage sag in a radial distribution system

2.2. Starting of the induction motors

The large induction motor start-up is another important factor that affects voltage sag [12]. The starting current during start-up of an induction motor is around 5 to 6 times that of current in the normal operation. In order to explain the start-up phenomenon, the schematic diagram during the induction motor start-up is illustrated in Fig. 2. In the figure, Z_S is the source impedance and Z_M is the motor impedance during the start-up period. The created voltage sag in the bus which supplies the motor and other loads can be computed from [12]:

$$V_{sag} = \frac{Z_M}{Z_S + Z_M} E \quad (2)$$

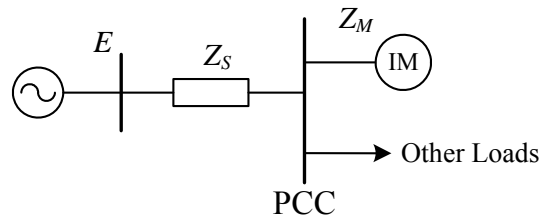


Fig. 2. The equivalent circuit of the induction motor for the study of voltage sag

2.3. Distribution transformer energization

When the distribution transformer is energized, the inrush current of the transformer is drawn from the network. The inrush current is firstly huge and after a while it decays and reaches to the small magnetizing current. In order to compute the maximum value of the inrush current and its consequent voltage sag, the equivalent of a single transformer is shown in Fig. 3 [13].

Considering Fig. 3, the maximum of inrush current $I_{Inrush\ max}$ should not exceed the following current:

$$I_{Inrush\ max} = \frac{1}{(X + X_P + X_{C,\min})} E \quad (3)$$

where X is the source Thevenin reactance at the bus of the energized transformer and $X_{C,\min}$ is the minimum magnetizing reactance of the transformer. The impedance $X_{C,\min}$ has typically the same value as $2(X_P + X_S)$ or $2X_T$. It is also assumed that X_T is the sum of the primary and secondary leakage reactances, and it is available from the transformer nameplate [13]. Assuming that the leakage reactances of the primary and secondary windings are equal, the maximum voltage sag can be computed from:

$$V_{sag} = \frac{X}{X + 2.5X_T} E \quad (4)$$

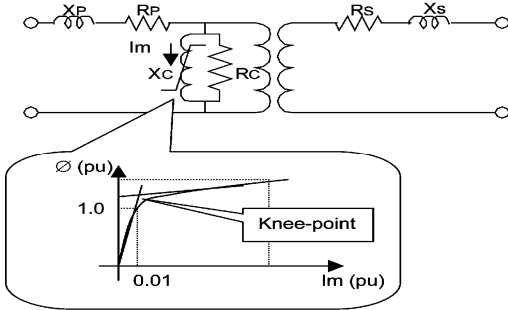


Fig. 3. Equivalent circuit of a single phase transformer [13]

3. The structure of D-Statcom and proposed control system

3.1. Structure of the D-Statcom

The three phase D-Statcom compensators are placed near and in parallel to the loads of distribution system. The main elements of the D-Statcom are shown in Fig. 4.

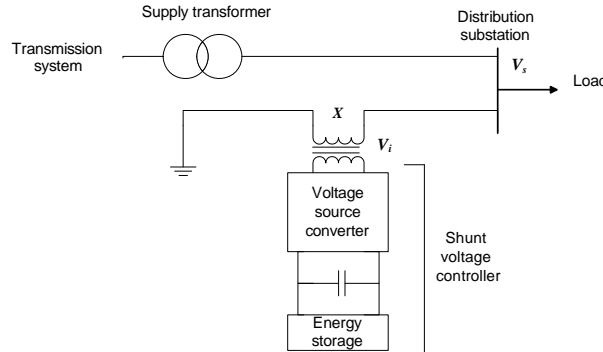


Fig. 4. Basic structure of the D-Statcom compensator

The D-Statcom compensator consists of DC capacitor, three phase inverter, coupling transformer, and block of control strategy. The main block in the structure of D-Statcom is voltage source inverter which converts the DC input voltage to a three phase voltage in the inverter output. As a result, the D-Statcom uses the inverter to create variable voltage source (in amplitude and phase) from the DC link voltage of the capacitor. Thus, the D-Statcom compensator absorbs or generates the reactive power using control system and stored energy.

3.2. Structure of the proposed controller

Different control strategies are used in the structure of D-Statcom that depends on the type of the used inverter. In this section based on the voltage source inverter, the proposed control strategy is presented.

3.2.1. Main control design of the proposed method

The D-Statcom consists of several gate controlled solid state power switches. The proposed method presented in this paper measures the active and reactive powers simultaneously to perform directly the switching process of the power electronic elements of the D-Statcom. The required signals for the gate are provided by the internal control of the inverter in response to the reference signals of the required active and reactive powers. The reference signals establish the main operation performance of the compensator and they are controlled by the external control via the operating signals and system variables. Fig. 5 show the performance of the internal control of the compensator.

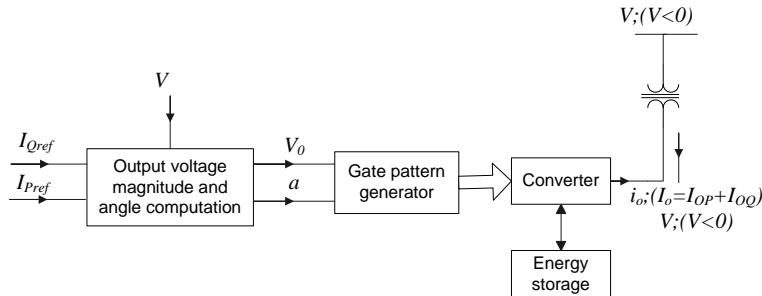


Fig. 5. Block diagram of the performance of the internal control of the D-Statcom compensator

The internal control is an essential part of the compensator. The main elements of the internal control are power switches of the inverter which produce the output voltage with the demanded magnitude and phase and the output is in synchronous with AC system. In this regard, the inverter can be considered as a synchronous voltage source behind a reactance. The magnitude and phase of this voltage source are controlled by the internal controller via appropriate reference signals. To do this, the internal control computes magnitude and phase of the demanded output voltage using I_{Qref} which obtained from the external control. As a result, the internal control produces a set of coordinated timing waveform. The magnitude and phase of the output voltage are two internal parameters that determine the active and reactive current of the inverter. In fact, these two parameters determine the active and reactive power exchanged with the systems. If the inverter is used only to exchange the reactive power, then the reference input of the input control is reactive power. From this situation, the input control infers magnitude and phase of the output voltage in order to provide the DC

voltage for the DC capacitor, because the value of the AC output voltage is directly proportional to the voltage of the DC capacitor.

3.2.2. Principles of the proposed control design

The block diagram representation of an internal voltage control for an inverter with the proposed internal control is shown in Fig. 6. The input signals for this system are bus voltage, V , inverter output current, I_Q , reactive reference current I_{Qref} and DC reference voltage V_{DC} . The DC voltage specifies the reactive power that should be provided by the inverter to supply its internal loss. As Fig. 6 shows the inverter output current is decomposed into active and reactive components. These components are compared with output reference reactive current and internal active reference current, respectively. The generated active and reactive error signals are amplified and then converted to the output voltage with the desired phase and magnitude. The error signals create the suitable signals proportional to phase reference obtained by phase locked loop (PLL) for driving the gate of the thyristors. It should be noted that the internal control design is able to drive an inverter with a DC power supply. In this case, the internal active reference current is added to the external active reference current and the result is the exchanged active power with the main AC grid. The combination of the internal and external active with the dominant demanded current determines magnitude and phase of the voltage, and the exchanged active and reactive power with main AC grid. The characteristic of desired terminal voltage versus output current of the compensator can be created with a minor control loop. This issue is shown in Fig. 7.

Finally, a signal proportional to the magnitude of the compensator current, I_Q with a specific polarity is obtained. Then, the obtained signal is added to reference voltage V_{Ref} . Therefore, the effective reference voltage V_{Ref}^* (which controls the voltage terminal) is obtained from:

$$V_{Ref}^* = V_{Ref} + k \cdot I_Q \quad (5)$$

where k is the regulation slop.

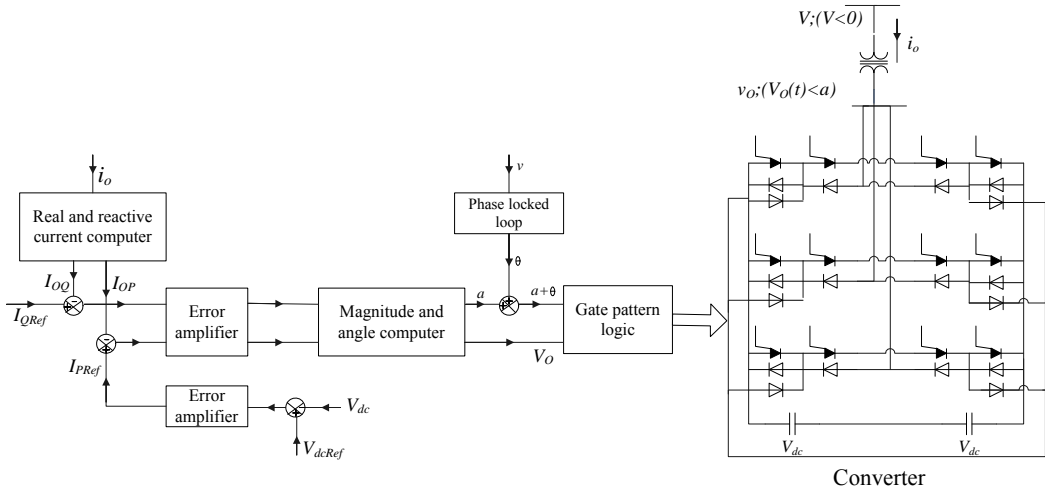


Fig. 6. The proposed control design for the D-Statcom compensator

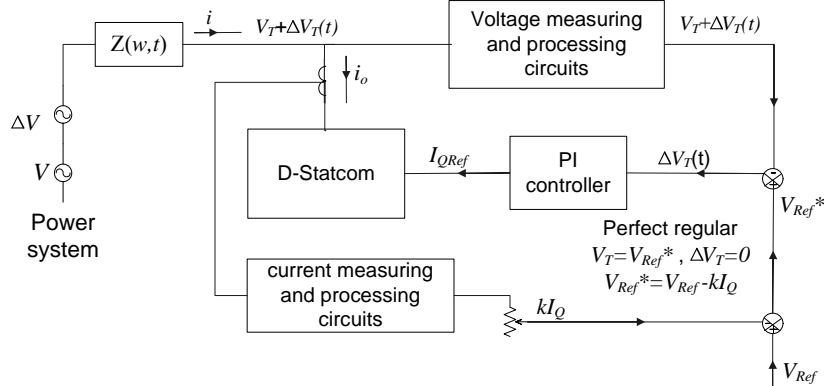


Fig. 7. Design control to consider the V-I characteristic in the static compensator

3.2.3. Transfer function and dynamic performance of D-Statcom

The dynamic performance in the normal range of operation is depicted in Fig. 8. This block diagram shows directly the principle of the control design of Fig. 7.

In the range of linear performance of the compensator and regarding Fig. 7, the terminal voltage of the compensator can be expressed in terms of internal voltage V and reference voltage V_{Ref} as follows:

$$V_T = V \cdot \frac{1}{1 + G_1 G_2 H X} + V_{Ref} \cdot \frac{G_1 G_2 X}{1 + G_1 G_2 H X} \quad (6)$$

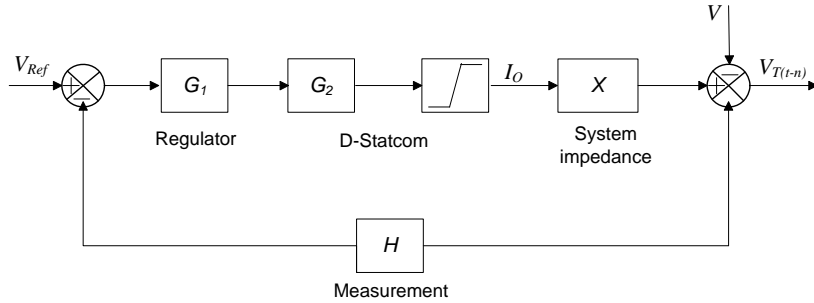


Fig. 8. Block diagram of transfer function of the D-Statcom compensator

Since the aim is to regulate the terminal voltage of the compensator against the system voltage, only small changes are considered. It is also assumed that $\Delta V_{Ref} = 0$. Thus, magnitude of the system voltage changes ΔV can be found from:

$$\frac{\Delta V_T}{\Delta V} = \frac{1}{1 + G_1 G_2 H X} = \frac{1}{1 + GHX} \quad (7)$$

where,

$$G_1 = \frac{1/k}{1 + T_1 s}, \quad G_2 = e^{-T_d s}, \quad H = \frac{1}{1 + T_2 s}, \quad G = G_1 G_2 = \frac{1/k}{1 + T_1 s} e^{-T_d s} \quad (8)$$

In the control design of the proposed method the following terms are defined:

T_1 = Main time constant of the PI controller

T_2 = Time constant of the measuring circuit of the amplitude

T_d = Transmission time transport of D-Statcom

k = Regulation slop

s = Laplace operator

4. System under study

In this part the factors that create the voltage sag in the distribution system are studied by simulating the IEEE 13-Bus standard test system using PSCAD/EMTDC software. In the simulation, the effect of D-Statcom compensator on voltage sag in the test system is studied. The standard test system is plotted in Fig. 9. For simplicity, the buses in Fig. 9 are shown by 3-digit numbers.

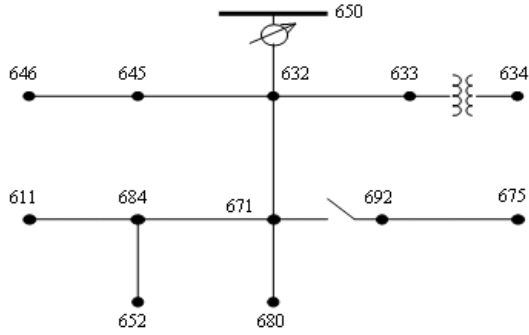


Fig. 9. Schematic diagram of the IEEE 13-Bus standard distribution system

In this figure, Bus 650 is chosen as the input bus to the system and it is fed by a 20kV voltage source. Also, a voltage regulator is placed between Buses 650 and 632. In the simulation of the voltage regulator, a transformer with on-load tap changer is used. To model the low voltage distribution system, a Y-Y 20kV/0.4kV transformer is employed. This transformer is located between Buses 633 and 634. It has rating apparent power of 500kVA with $R=1.1\%$ and $X=2\%$. Other specifications of the equipments used in the test system are given in [14].

5. Simulation results

In this section, the factors that create voltage are simulated. As previously mentioned, the factors are short circuit faults, starting of induction motors and energizing the distribution transformers. After simulating these factors, the compensation of the created voltage sag using D-STATCOM is studied. The D-STATCOM is placed on Bus 671 of the test system.

5.1. Investigation of short circuit faults

In the simulation, firstly, different short circuits are created on Bus 671. Then, the voltage changes of the other buses due to these short circuits are obtained. After that, the D-STATCOM compensator with the proposed direct control is employed to show the improvement in the voltage profile. The time period of the simulation for this situation is 2 seconds. Also, the faults occur in $t_s=1\text{sec}$, and it is removed after 0.1sec. In the simulations of this part, the fault impedance is 1.0Ω and the fault resistance between the lines is 0.1Ω . In the simulation, two types of the short circuits are considered for Bus 671. The faults are single phase to ground and three phase short circuits. The results are obtained where there is no D-STATCOM. The results then compared with results of the case when the D-STATCOM is present. The voltage profiles of Bus 611 due to two type short circuits in Bus 671 without and with D-STATCOM are shown in Figs. 10 and 11, respectively.

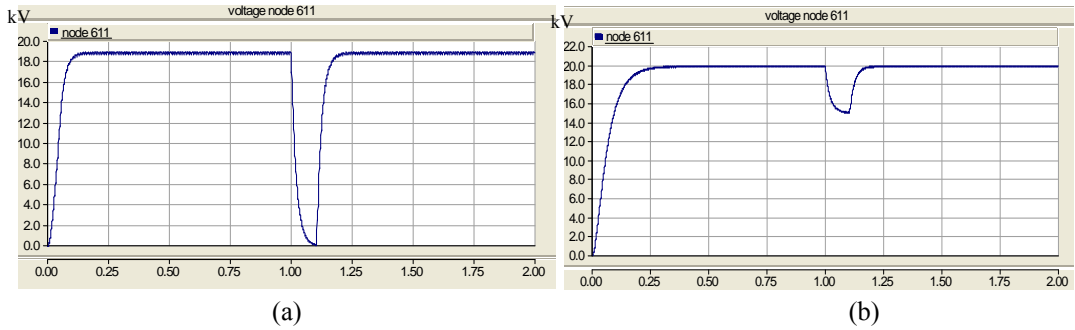


Fig. 10. Voltage variations in Bus 611 due to short circuit in Bus 671 without D-Statcom compensator, a) Three phase short circuit; b) Single phase to ground short circuit

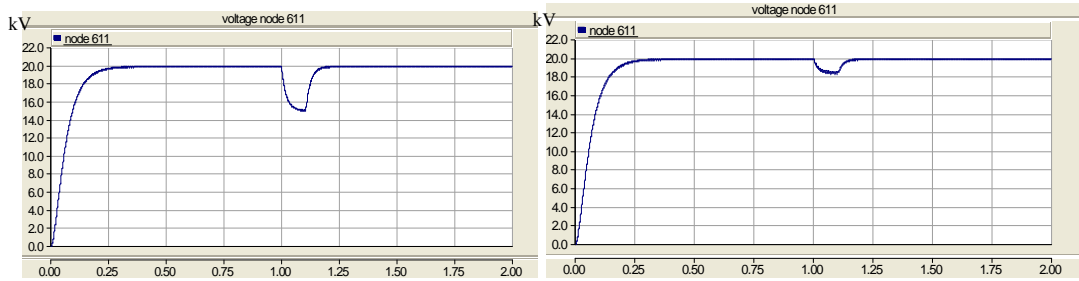


Fig. 11. Voltage variations in bus 611 due to short circuit in bus 671 with d-statcom compensator, a) three phase short circuit, b) single phase to ground short circuit

The results of the simulation for symmetrical and unsymmetrical faults (which occurs at Bus 671) in the compensated and uncompensated system are shown in Tables 1 and 2, respectively. In these tables, the magnitude of the voltages are given for different short circuits. In addition, in order to show the capability of the proposed control method, the method is compared with the d-q compensated system.

To compare the results, the term of d is employed which represents the deviation of the voltage from the rating value of the voltage. When Figs. 10 with 11, and Tables 1 with 2 are compared, then it can be found that in the cases when the magnitude of the voltages are in the range of $d < 0.1$ and $0.3 < d < 0.6$, the voltage sags due to the short circuits are reduced by 100%. In addition, the magnitude of the faults lie in the range of $0.6 < d < 0.9$. Thus, this reduces the impacts due to voltage sag. As a result, compensation using D-Statcom leads to power quality improvement with the amount of 55.84%. Also, it can be found from Table 2 that the proposed control method compared to conventional d-q compensated system, the voltage sage is reduced to a value lies in the range of 5% to 18%.

It is also worthwhile to note that, the D-Statcom compensator is capable to provide the energy which is needed for compensation of the unsymmetrical and

symmetrical faults. For example, if the fault is cleared before 75msec, the compensator can compensate perfectly the voltage interruption by injecting the active and reactive powers. In this situation, the D-STATCOM performs its compensation using its stored energy as well as entering to the mode of minimum active power injection. Fig. 12 shows the voltage variations of Buses 611 and 675 due to three phase short circuit at Bus 671. Therefore, the voltage profile in the compensated system is greater than the threshold of voltage sag and in this case the compensation is perfectly performed.

Table 1
The magnitude of bus voltages due to different short circuits (occurs at Bus 671) in the uncompensated system (in kV)

Kind of short circuit \ Bus number	650	634	646	675	611
Single phase to ground short circuit	19.950	0.390	19.636	17.233	17.190
Phase to Phase short circuit	19.972	0.373	18.791	10.579	10.470
Double phase to ground fault	19.967	0.370	18.656	9.791	9.669
Three phase short circuit	20.014	0.319	17.701	0.141	0.126
Three Phase to ground short circuit	19.995	0.354	17.830	0.385	0.1283

Table 2
The magnitude of bus voltages due to different short circuits (occurs at Bus 671) in the D-STATCOM compensated system (in kV)

Kind of short circuit \ Bus number	Control system	650	634	646	675	611
Single phase to ground short circuit	Proposed control	19.951	0.381	19.164	18.403	18.399
	d-q control	18.813	0.362	18.128	17.282	17.285
Phase to Phase short circuit	Proposed control	19.950	0.372	18.751	17.687	17.684
	d-q control	18.685	0.354	17.528	16.692	16.685
Double phase to ground fault	Proposed control	19.949	0.364	18.333	16.862	16.859
	d-q control	18.672	0.342	17.223	16.121	16.124
Three phase short circuit	Proposed control	19.966	0.347	17.462	15.130	15.127
	d-q control	18.413	0.321	16.125	13.248	13.252
Three Phase to ground short circuit	Proposed control	19.956	0.347	17.450	15.125	15.125
	d-q control	17.297	0.318	15.879	12.412	12.627

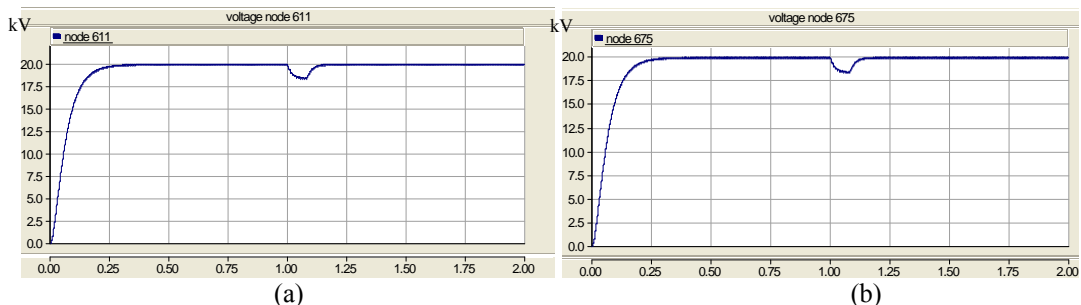


Fig. 12. Voltage variation of a) Bus 611 and b) Bus 675 due to three phase to ground short circuit at Bus 671 considering compensating voltage interruptions

5.2. Investigation of induction motor start up

In this situation, the role of the D-Statcom in the process of induction motor start-up is simulated. In this regard, a 150hp, 3554rpm, 20kV, 60Hz three phase induction motor is connected to Bus 671 [14]. The time duration of the simulation is assumed 2 sec and after 1 sec, the motor is connected to the bus by using the motor control switch and the motor is started in the speed control.

The voltage variations of buses 611 and 675 due to start-up of the induction motor for two cases of uncompensated system and compensated system are depicted in figs. 13 and 14, respectively. comparison of these figures shows that when the compensator with the proposed direct control is used, the voltage sag due to the starting current of induction motor is reduced considerably. The results of the comparisons are given in table 3. It can be found from this table that with the use of the compensator, the voltage profile is firstly increased by 12.78% then it returns to the value of 0.965p.u (19.317kv) of the base voltage. This issue shows that the compensation is performed perfectly.

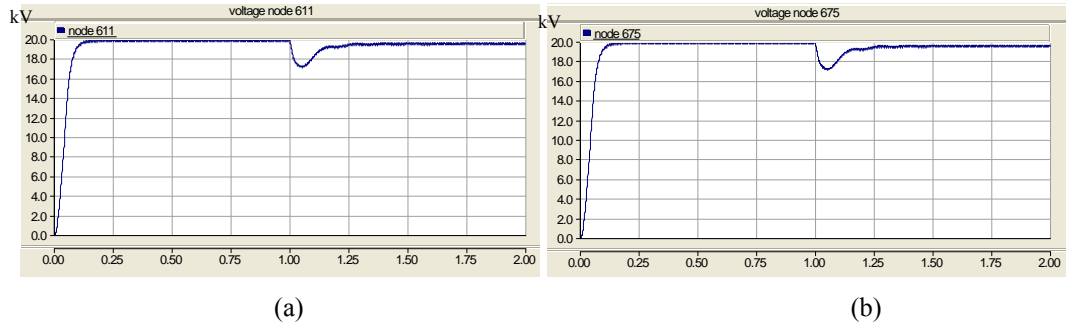


Fig. 13. Voltage variation at a) Bus 611, b) at Bus 675 due to starting of the induction motor (at Bus 671) in the uncompensated system

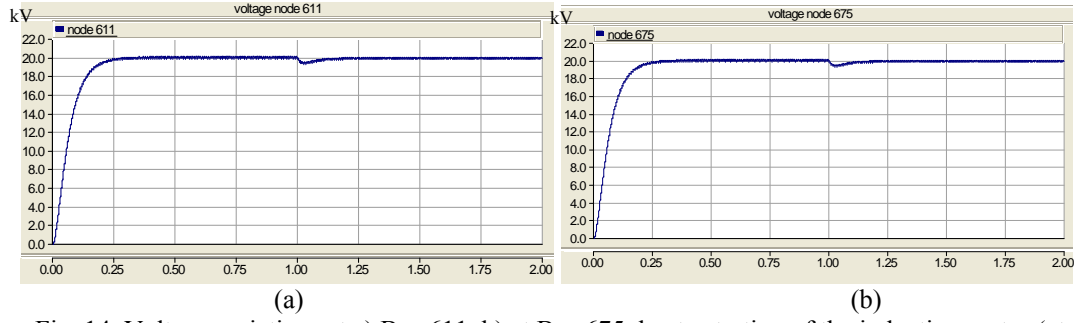


Fig. 14. Voltage variations at a) Bus 611, b) at Bus 675 due to starting of the induction motor (at Bus 671) in the compensated system

Table 3

The percentage of voltage improvement in the case of starting induction motor (at Bus 671) due to use of D-STATCOM compensator

State	Bus number	675	611
Uncompensated system		17.266kV	17.264kV
Compensated system		19.320kV	19.317kV
At Bus 671		12.77%	12.78%

5.3. Investigation of transformer energization

Regarding the topology of the network, a low voltage transformer is connected to Bus 634. In simulation, a switch is used for energizing the transformer and it is closed at $t=1\text{sec}$. Fig. 15 shows the voltage variation at Bus 646 due to the transformer energization at Bus 634. As Fig. 15 shows due to being small power of the transformer, only Buses 633 and 632 are greatly affected by this energization and other parts of the transformer are less affected by this issue. Also, the results of the simulating for compensation of voltage sag due to transformer energization are shown in Fig. 16. The comparison between compensated and uncompensated system are given in Table 4. As this table shows when the compensator is used, the voltage profile is improved by about 13.6%. This shows that use of D-STATCOM, the voltage sag decreased remarkably

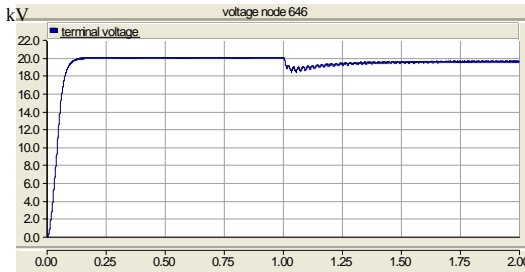


Fig. 15. Variation of voltage at Bus 646 due to transformer energization at Bus 634

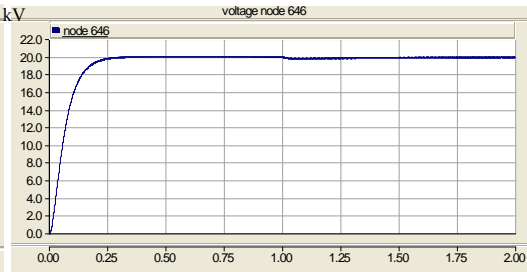


Fig. 16. Voltage compensation at Bus 646 due to transformer energization at Bus 634

Table 4

The percentage of voltage improvement in the case of transformer energization (at Bus 634) due to use of D-STATCOM compensator

State	Bus number	675	611
Uncompensated system		17.412kV	17.403kV
Compensated system		19.781kV	19.777kV
Percentage of voltage improvement		13.66%	13.64%

6. Conclusions

In this paper, a method called direct control is presented to reduce the voltage sag in distribution system. The proposed method is simultaneously employed to control directly the switching patterns of power electronic switches of the D-Statcom. Finally, the compensator injects power proportional to the network disturbance to improve the voltage profile. In order to validate the proposed method in reducing voltage sag, the effects of D-Statcom for different cases are simulated on the IEEE 13-Bus standard test system. The results of the simulation indicate that the compensator with the proposed control is capable in reducing the voltage sag in the case of occurring several situations including short circuit faults, induction motor start-up and transformer energization.

R E F E R E N C E S

- [1]. *J.A. Martinez, J. Martin-Arnedo*, Voltage Sag Studies in Distribution Networks—Part II: Voltage Sag Assessment, in IEEE Trans. Power Delivery, **vol. 21**, no. 3, 2006, pp. 1679-1688
- [2]. *J.A. Martinez, J. Martin-Arnedo*, Voltage Sag Studies in Distribution Networks—Part I: System Modeling, in IEEE Trans. Power Delivery, **vol. 21**, no. 3, 2006, pp. 338-345
- [3]. *IEEE Std. 1159-1995*, IEEE Recommended Practice for Monitoring Electric Power Quality, Technical report, in The Institute of Electrical and Electronics Engineers, Inc, 1995.
- [4]. *P. Heine, M. Khronen*, Voltage Sag Distributions Caused by Power System Faults, in IEEE Trans. Power Systems, **vol. 18**, no. 4, 2003, pp. 1367-1373
- [5]. *N. Golovanov, G.C. Lazaroiu*, Effects of Symmetrical and Unsymmetrical Sags on Induction Motors, in U.P.B. Sci. Bull., Series C, **vol. 68**, no. 2, 2006, pp. 63-78
- [6]. *R. Mineski, R. Pawelek, I. Wasik*, Shunt Compensation for Power Quality Improvement Using a Statcom Controller: Modeling and Simulation, in IEE Proc. Generation, Transmission and Distribution, **vol. 151**, no. 2, 2004, pp. 274-280
- [7]. *S.R. Nam, J.M. Sohn, S.H. Kang, J.K. Park*, Ground-Fault Location Algorithm for Ungrounded Radial Distribution Systems, in Journal of Electrical Engineering, **vol. 89**, no. 6, 2007, pp. 503-508
- [8]. *Y.H. Song, A.T. Johns*, Flexible AC Transmission Systems (FACTS), in IEEE Press, New York, 1999
- [9]. *H. Masdi, N. Mariun, S. Mahmud, A. Mohamed, S. Yusuf*, Design of a Prototype D-statcom for Voltage Sag Mitigation, in IEEE National Power and Energy Conf., 2004, pp. 61-66
- [10]. *B. Blazic, I. Papic*, Improved D-Statcom Control for Operation with Unbalanced Currents and Voltages, in IEEE Trans. Power Delivery, **vol. 21**, no. 1, 2006, pp. 225-233
- [11]. *C. Radhakrishna, M. Eshwardas, G. Chebiyam*, Impact of Voltage Sag in Practical Power System Network, in IEEE/PES Conference, **vol. 1**, 2001, pp. 567-572
- [12]. *M.H.J. Bollen*, Understanding Power Quality Problems- Voltage Sags and Interruptions, IEEE Press, New York, 2000
- [13]. *M. Nagpal, T.G. Martinich, A. Moshref, K. Morison, P. Kundur*, Assessing and Limiting Impact of Transformer Inrush Current on Power Quality, in IEEE Trans. Power Delivery, **vol. 21**, no. 2, 2006, pp. 890-896
- [14]. *W.H. Kersting*, Radial distribution test feeders, in Power Engineering Society Winter Meeting, 2001. **vol. 2**, 2001, pp. 908-912.